



## Original article

# Synthesis, cytotoxicity and molecular modelling studies of new phenylcinnamide derivatives as potent inhibitors of cholinesterases



Aamer Saeed<sup>a</sup>, Parvez Ali Mahesar<sup>a</sup>, Sumera Zaib<sup>b</sup>, Muhammad Siraj Khan<sup>b</sup>, Abdul Matin<sup>c</sup>, Mohammad Shahid<sup>d</sup>, Jamshed Iqbal<sup>b,e,\*</sup>

<sup>a</sup> Department of Chemistry, Quaid-I-Azam University, Islamabad 45320, Pakistan

<sup>b</sup> Centre for Advanced Drug Research, COMSATS Institute of Information Technology, Abbottabad 22060, Pakistan

<sup>c</sup> Institute of Biomedical and Genetic Engineering, PO Box 2891, Sector G-9/1, Islamabad, Pakistan

<sup>d</sup> Department of Bioinformatics, Fraunhofer Institute SCAI, Sankt Augustin, Germany

<sup>e</sup> Department of Pharmaceutical Sciences, COMSATS Institute of Information Technology, Abbottabad 22060, Pakistan

## ARTICLE INFO

## Article history:

Received 12 October 2013

Received in revised form

15 February 2014

Accepted 6 March 2014

Available online 7 March 2014

## Keywords:

Phenylcinnamide derivatives

Alzheimer's disease

Cholinesterases inhibitors

Cytotoxicity

Molecular docking

## ABSTRACT

The present study reports the synthesis of cinnamide derivatives and their biological activity as inhibitors of both cholinesterases and anticancer agents. Controlled inhibition of brain acetylcholinesterase (AChE) and butyrylcholinesterase (BChE) may slow neurodegeneration in Alzheimer's diseases (AD). The anticholinesterase activity of phenylcinnamide derivatives was determined against *Electric Eel* acetylcholinesterase (EeAChE) and horse serum butyrylcholinesterase (hBChE) and some of the compounds appeared as moderately potent inhibitors of EeAChE and hBChE. The compound 3-(2-(Benzyloxy)phenyl)-N-(3,4,5-trimethoxyphenyl)acrylamide (**3i**) showed maximum activity against EeAChE with an  $IC_{50}$   $0.29 \pm 0.21$   $\mu$ M whereas 3-(2-chloro-6-nitrophenyl)-N-(3,4,5-trimethoxyphenyl)acrylamide (**3k**) was proved to be the most potent inhibitor of hBChE having  $IC_{50}$   $1.18 \pm 1.31$   $\mu$ M. To better understand the enzyme–inhibitor interaction of the most active compounds toward cholinesterases, molecular modelling studies were carried out on high-resolution crystallographic structures. The anticancer effects of synthesized compounds were also evaluated against cancer cell line (lung carcinoma). The compounds may be useful leads for the design of a new class of anticancer drugs for the treatment of cancer and cholinesterase inhibitors for Alzheimer's disease (AD).

© 2014 Elsevier Masson SAS. All rights reserved.

## 1. Introduction

Acetylcholine (ACh) is a cholinergic neurotransmitter, released presynaptically by cholinergic terminals, and it interacts with either nicotinic or muscarinic receptors thereby affecting function of postsynaptic cells. Signalling action of ACh is terminated by the action of acetylcholinesterase (AChE) and butyrylcholinesterase (BChE) [1,2]. Both enzymes are widely distributed throughout the body; however, AChE remains the major cholinesterase within the human brain. All the brain parts that are innervated by cholinergic transmission in a normal brain hold AChE and BChE activity [3].

Alzheimer's disease is a long lasting neurodegenerative disorder that brings about irreversible memory loss in elderly individuals. Furthermore, this disease has not only been reported of having

defined accumulation of amyloid- $\beta$  peptide plaques at extracellular level but also characterized with the intracellular neurofibrillary tangles (NFTs) in the brains of suffering patients. With the progression of disease, the prominent indications are the continuous memory loss, confusion, petulance, anger and the lack of vigour in body to function evenly which eventually become the ultimate cause of death [4–6]. It is estimated that 24.3 million people were suspected to have Alzheimer's disease (AD) in 2005; also the projected number of individuals with AD at world level in 2020 and in 2040 would be 42.3 and 81.1 million, respectively [7]. In this situation, global escalating occurrence of AD has compelled researchers to undertake studies on neurodegenerative disorders (NDDS) [8].

Cholinesterases belong to a family of serine hydrolases that split acetylcholine into choline and acetic acid, an unavoidable step in retaining the function of cholinergic neuron [9]. AChE has five important regions within active site and these are important to understand substrate and inhibitor binding pattern. These regions are, 1) catalytic triad residues, 2) acyl pocket, 3) oxyanion hole, 4) anionic site (AS), 5) and a peripheral anionic site (PAS) [10–15]. The

\* Corresponding author. Centre for Advanced Drug Research, COMSATS Institute of Information Technology, Abbottabad 22060, Pakistan.

E-mail addresses: [drjamshed@ciit.net.pk](mailto:drjamshed@ciit.net.pk), [jamshediqb@gmail.com](mailto:jamshediqb@gmail.com) (J. Iqbal).

AChE binds to PAS resulting in the formation of amyloid- $\beta$  peptide plaques and acetylcholinesterase inhibitors (AChEIs) bind to the PAS to prevent amyloid- $\beta$  peptide plaques formation [16,17]. However, such treatment (using AChEIs) only relieves the symptoms for short term and do not eradicate the disease eternally [18]. The major role of acetylcholinesterase (AChE) is to catalyze the hydrolysis of acetylcholine (ACh) in cholinergic synapses and replacement of AChE function in Alzheimer's brains [19]. Some of the important cholinesterase inhibitors which are employed in the treatment of AD are rivastigmine, galantamine, tacrine, ensaculin and donepezil. Among these remedies the rivastigmine is broader in its action as it non-specifically inhibits AChE as well as BChE, whereas galantamine and donepezil specifically inhibit AChE thus increasing ACh level at neuronal level and relieving AD symptoms but they all cannot stop progress of dementia [20]. Various compounds like carbamates (e.g., neostigmine and physostigmine etc), organophosphates, coumarine and cinnamide derivatives are reported in literature as inhibitors of cholinesterases [18,21,22]. Apart from anticholinesterase and cytotoxic activity cinnamide derivatives (N-(carboxyaryl)-phenylcinnamide) have shown their activity against leukotriene B<sub>4</sub> (LTB<sub>4</sub>), which is a metabolic product of arachidonic acid and a potent inflammatory mediator [23,24]. LTB<sub>4</sub> has important role in a range of diseases, like psoriasis, adult respiratory distress syndrome, inflammatory bowel disease and rheumatoid arthritis, it makes cinnamide derivatives as potent therapeutic agents against inflammatory disorders [25–29].

The aim of the present study was to synthesize and investigate phenylcinnamide derivatives as anticholinesterase as well as anti-cancer agents.

## 2. Results and discussion

### 2.1. Chemistry

We envisioned that Doebner–Knoevenagel condensation was the best available route to synthesize cinnamic acids derivatives (**1**) (**a–y**) [30,31]. It was subsequent one pot activation and coupling which led to formation of corresponding amides with 2,4,6-trichloro-1,3,5-triazine [32] that ultimately afforded the desired products phenylcinnamide (**3a–y**) in a good to excellent yield. Gratifyingly, we came to know that cyanuric chloride (TCT) was cost-effective and stable reagent for amide formation, more importantly it was easily handled and transformation took place at

**Table 1**  
Inhibitory potential of phenylcinnamide derivatives against EeAChE and hBChE.

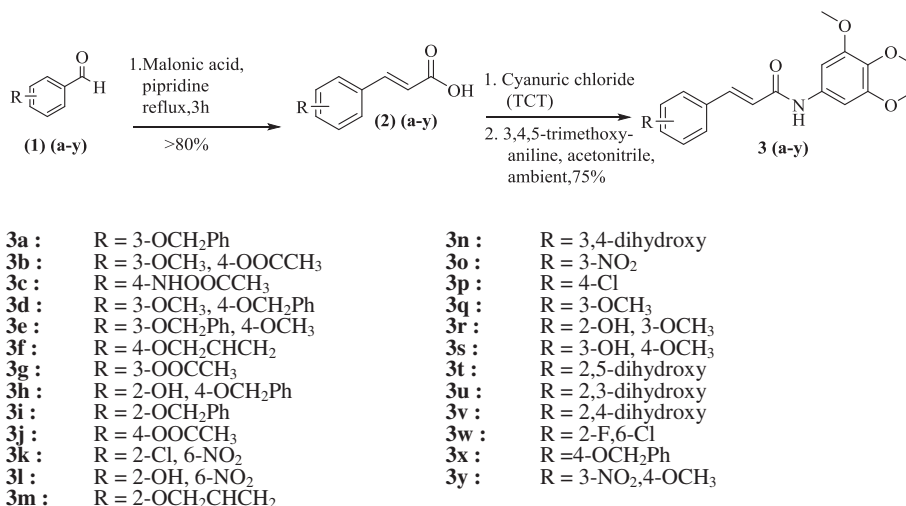
Compounds	EeAChE	hBChE
	IC <sub>50</sub> ± <sup>a</sup> SEM (μM)/(%Inhibition)	
<b>3a</b>	6.52 ± 0.39	3.93 ± 1.44
<b>3b</b>	4.98 ± 0.27	(31.1)
<b>3c</b>	12.54 ± 0.65	3.85 ± 0.91
<b>3d</b>	12.61 ± 1.48	(32.8)
<b>3e</b>	6.02 ± 2.95	(31.1)
<b>3f</b>	(33.6)	(32.6)
<b>3g</b>	(29.2)	1.25 ± 0.08
<b>3h</b>	1.59 ± 1.45	(27.2)
<b>3i</b>	0.29 ± 0.21	(32.1)
<b>3j</b>	(36.5)	(37.4)
<b>3k</b>	(34.2)	1.18 ± 1.31
<b>3l</b>	12.77 ± 1.06	(35.4)
<b>3m</b>	1.41 ± 0.77	(24.8)
<b>3n</b>	(36.4)	(34.6)
<b>3o</b>	3.24 ± 2.16	(26.2)
<b>3p</b>	(31.2)	(25.7)
<b>3q</b>	12.91 ± 0.98	(41.8)
<b>3r</b>	6.22 ± 0.33	5.19 ± 0.78
<b>3s</b>	4.22 ± 0.03	7.65 ± 0.51
<b>3t</b>	(30.3)	(36.2)
<b>3u</b>	(31.2)	(41.2)
<b>3v</b>	(36.6)	(18.21)
<b>3w</b>	(34.1)	1.32 ± 0.15
<b>3x</b>	3.72 ± 0.13	(33.5)
<b>3y</b>	6.69 ± 4.0	(28.1)
<b>Neostigmine</b>	22.0 ± 3.01	49.1 ± 6.0
<b>Donepezil</b>	0.03 ± 0.003	6.37 ± 0.32

<sup>a</sup> SEM shows standard error of mean of three experiments.

ambient temperature. All of the synthesized compounds were characterized with <sup>1</sup>H and <sup>13</sup>C NMR along with IR (Scheme 1).

### 2.2. In vitro inhibition studies of EeAChE and hBChE

*In vitro* inhibitory studies of synthesized phenylcinnamide derivatives were carried out on EeAChE and hBChE. Inhibition potency of compounds expressed as IC<sub>50</sub> values is shown in Table 1. Among the phenylcinnamide derivatives, **3i** showed maximum inhibitory activity against EeAChE because of its electron donating benzyloxy (–OCH<sub>2</sub>Ph) group at *ortho* position, although the same group attached to *meta* and *para* position showed little activity. However, when –OCH<sub>2</sub>CHCH<sub>2</sub> group was attached to the same *ortho* position then a decrease in the activity of the compound (**3m**) was observed,



**Scheme 1.** Synthesis of substituted phenylcinnamide derivatives.

same was the case when  $-\text{OCH}_2\text{CHCH}_2$  group was attached to the same *para* position (**3f**). In addition, the value of  $\text{IC}_{50}$  further decreased when a  $-\text{NO}_2$  group was attached at the *meta* position to the benzene ring (**3o**). Introduction of two hydroxy substituents to benzene ring further decreased inhibition against the EeAChE for **3n**, **3t**, **3u** and **3v**. As for as the action of the phenylcinnamide derivatives against the hBChE was concerned, **3k** having  $-\text{Cl}$  and  $-\text{NO}_2$  groups at *ortho* positions exhibited maximum inhibitory potency against hBChE. The attachment of the  $-\text{OOCCH}_3$  group instead of  $-\text{Cl}$  and  $-\text{NO}_2$  groups (**3g**) to the *meta* position slightly reduced the inhibitory potency. Electron withdrawing groups like  $-\text{Cl}$  and  $-\text{F}$  simultaneously at *ortho* positions, as in case of compound **3w** also resulted in potent inhibitor of hBChE but relatively less potent than **3k** and **3g**.

### 2.3. Cytotoxicity of 3 (a–y) against lung carcinoma (H157) cells

In the present study we investigated the toxic effects of these compounds (in dose dependent manner) against lung carcinoma (H157) cells through SRB assay in order to assess their behaviours. The vincristine a standard anticancer drug was used as reference for comparison to the test compounds. In the present study, at  $1\ \mu\text{M}$  end concentration in the experiment, **3w** and **3y** demonstrated almost 66% cytotoxicity, exhibiting highest antiproliferative activities. Compounds **3e** and **3t** were the next most potent compounds showing about 61% and 60% cytotoxicity respectively at the same concentration ( $1\ \mu\text{M}$ ). The Fig. 1 reveals the cytotoxic effects of phenylcinnamide derivatives against lungs cancer cells. Antiproliferative activity of the positive control vincristine towards lung carcinoma (H157) cell line was about 46% at final concentration of  $100\ \mu\text{M}$ , whereas the result revealed that these compounds were many folds potent in comparison to positive control. Therefore, it is shown that phenylcinnamide derivatives exhibited more cytotoxic effects than standard anticancer drug (vincristine) even at lowest tested concentration.

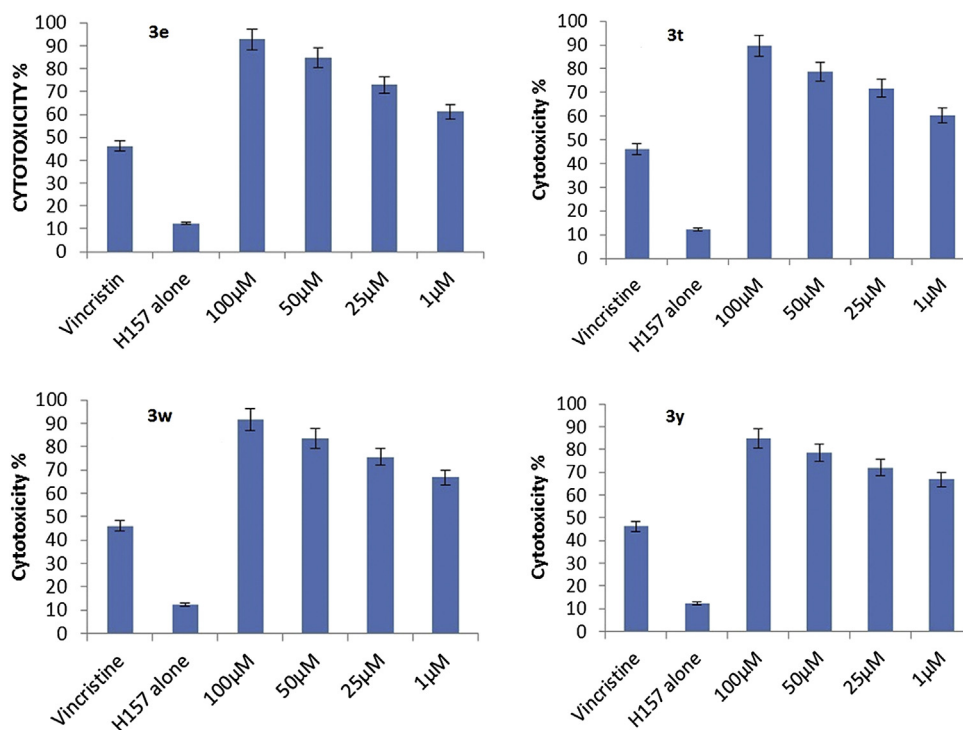


Fig. 1. Antiproliferative activity of the synthesized phenylcinnamide derivatives towards lung carcinoma (H157) cell line at various concentrations. Vincristine was used as standard drug ( $100\ \mu\text{M}$ ).

### 2.4. Docking and pose ranking

To investigate possible ligand–AChE interactions, docking studies were performed to generate binding modes. For acetylcholinesterase, the compounds were docked to TcAChE (*Torpedo californica* PDB Code: 3I6Z) and for butyrylcholinesterase a high-resolution crystal structure of  $2.00\ \text{\AA}$  huBChE (human PDB Code: 1P0I) was selected for docking studies. The results of re-docking experiments showed that the structures were well prepared and the docking program reproduced the natively bound conformations of the co-crystallized bound ligands. An RMSD of  $1.80\ \text{\AA}$  was obtained for the re-docked ligand (galantamine) of TcAChE that indicated a good prediction by the docking program. However, the re-docking experiment of using galantamine as a reference ligand in huBChE did not produce satisfactory results in terms of RMSD, however, the orientation of the predicted conformation of the re-docked structure was flipped at  $180^\circ$  that resulted in larger RMSD values of  $8\ \text{\AA}$  and higher.

Similarly, the docking results for these compounds **3 (a–y)** were obtained for both enzymes, which showed that there were different conformations (poses) predicted for each compound. Table 2 shows the docking scores obtained with LeadIT and the rank number of best pose obtained with NNScore algorithm for the compounds screened against both TcAChE and huBChE enzymes. Docking scores of the compounds range from  $-20$  to  $-39$  for both enzymes, however, filtering the poses for the compounds by NNScore showed there could be other conformations that might interact favourably with the enzymes. The docking scores for the first conformation and the selected conformation ranks are given in Table 2.

### 2.5. Binding mode analysis

A common binding mode was observed for the all these compounds docked into both structures of TcAChE and huBChE enzymes. The compounds interact in a similar way like the reference

**Table 2**  
Docking scores and best pose ranks for the compounds screened against TcAChE and huBChE.

Compound	Docking scores (kcal/mol)		Pose ranks in top 10	
	TcAChE	huBChE	TcAChE	huBChE
<b>3a</b>	-27.25	-35.69	10	2
<b>3b</b>	-34.52	-25.07	6	7
<b>3c</b>	-31.38	-39.34	9	8
<b>3d</b>	-28.43	-25.75	4	8
<b>3e</b>	-28.66	-31.62	9	3
<b>3f</b>	-26.38	-22.25	7	7
<b>3g</b>	-34.07	-28.15	10	6
<b>3h</b>	-29.81	-26.19	3	1
<b>3i</b>	-30.16	-25.57	1	4
<b>3j</b>	-31.09	-27.63	10	8
<b>3k</b>	-36.33	-29.52	7	6
<b>3l</b>	-27.13	-21.52	7	2
<b>3m</b>	-26.18	-28.91	6	3
<b>3n</b>	-35.64	-30.99	6	4
<b>3o</b>	-33.44	-39.59	3	1
<b>3p</b>	-25.11	-20.57	6	2
<b>3q</b>	-26.89	-25.72	2	10
<b>3r</b>	-29.13	-27.03	4	4
<b>3s</b>	-27.60	-26.89	8	1
<b>3t</b>	-28.70	-28.24	5	5
<b>3u</b>	-30.83	-28.80	10	10
<b>3v</b>	-29.41	-26.19	10	10
<b>3w</b>	-25.83	-24.31	5	3
<b>3x</b>	-27.78	-28.05	7	9
<b>3y</b>	-33.32	-32.67	5	4

ligand galantamine as shown in Figs. 2 and 3. In both enzymes, the predicted docked conformations of the compounds adapt similar orientations and form exactly the same interactions with the active site residues. As shown in Table 2, the poses with preferred binding modes that are selected by the external scoring functions occupy the active site of the enzyme and interact with the same residues in both enzymes. Therefore, the preferred binding modes selected by external scoring function were in accordance to the interactions made by the reference ligand galantamine in the active site of TcAChE as shown in Figs. 2 and 3. As it appears in Fig. 2, the trimethoxybenzoic moiety of the compounds is involved with hydrogen bond interaction with Ser200, that is anchored between Trp233 and Trp84 and the benzene ring is making aromatic stacking interactions with Phe290. Tyr121 is involved in both hydrogen bonding interactions as well as in aromatic interactions with the phenyl moiety. The tails of the compounds are positioned in the opening of the enzyme pocket and adapt flexible

conformations and is involved in a variety of interactions in which the interaction with Trp279 is common. The hydrogen bond networks formed by most of the compounds include hydrogen bonding with Tyr70, Tyr121 and Ser200 in TcAChE.

## 2.6. Molecular dynamics simulations

In total, 50 individual molecular dynamics simulations were conducted for all the selected poses of the compounds against both enzyme structures of TcAChE and huBChE. Each enzyme–ligand complex was parameterized for the high-ranking pose filtered and selected by the external scoring function NNScore. The pre-equilibration steps of density and final equilibration results (Figs. 4 and 5) showed that the complexes were equilibrated well, and the protein–ligand complexes can be further simulated to obtain enough samples for computing free energy of binding values as well as determine the stability of the binding modes. Fig. 6 shows the RMSD deviations of ligand atoms in the production MD runs of 5ns simulation time. The ligand atoms of all compounds do not show deviations during the simulation time and suggests that the predicted docked conformations remain stable during the simulation and the selected binding poses are favoured inside the active site pockets of the enzymes.

## 2.7. Calculations of binding free energy

The binding free energies ( $\Delta G$ ) were estimated by using Mechanics/Poisson–Boltzmann Surface Area (MM/PBSA) method for all compounds against both TcAChE and huBChE enzymes, the values are given in Table 3. The estimated  $\Delta G$  values showed that the activities of compounds predicted against TcAChE are higher as compared to huBChE enzyme for most of the compounds. However, some of the compounds have similar binding energies estimated for both enzymes. The observed correlation of estimated  $\Delta G$  and experimental  $\Delta G$  is positive (i.e. 0.41) for TcAChE but no correlation is observed between the experimental and estimated  $\Delta G$  for huBChE (i.e. correlation of 0.02). The reason for observing no correlation in the case of huBChE enzyme may be the structural differences between the horse BChE and human BChE enzymes. These results show that MM/PBSA based method to systematically evaluate free energy of binding for a series of compounds can predict satisfactorily the relative binding free energies when the modelling and experimental evaluation is performed on the same structures.

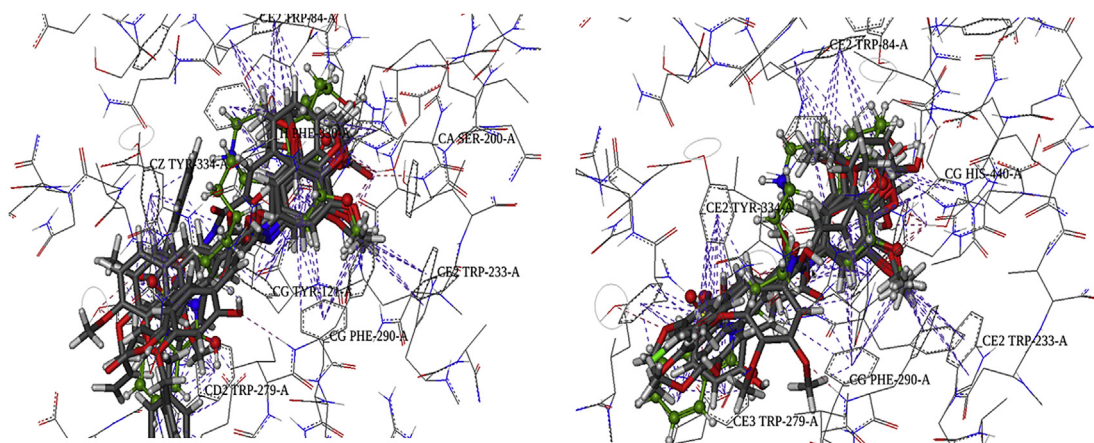


**Fig. 2.** Preferred binding modes for the compounds docked into the active site pocket of TcAChE. (Left): Predicted conformations of compounds **3e**, **3f**, **3g**, **3h**, **3i** and **3j** shown in CPK model. The reference ligand Galantamine (G6X) is shown in green. (Right): Predicted conformations of compounds **3p**, **3q**, **3r**, **3s**, **3t** inside the active site of TcAChE. Compounds are shown in CPK model and the reference ligand Galantamine is shown in green colour. (For interpretation of the references to colour in this figure legend, the reader is referred to the web version of this article.)

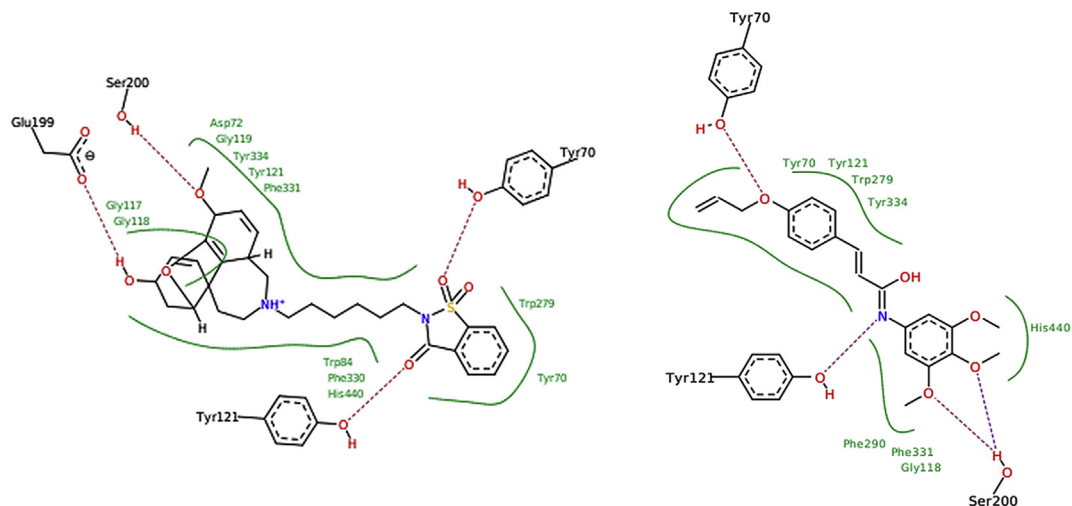


**Fig. 3.** Interaction diagrams of reference ligand (Galantamine, left) and compound **3f** (right). Hydrogen bond interactions are shown with red dotted lines and hydrophobic interacting residues are shown in the regions surrounding by green lines. (For interpretation of the references to colour in this figure legend, the reader is referred to the web version of this article.)

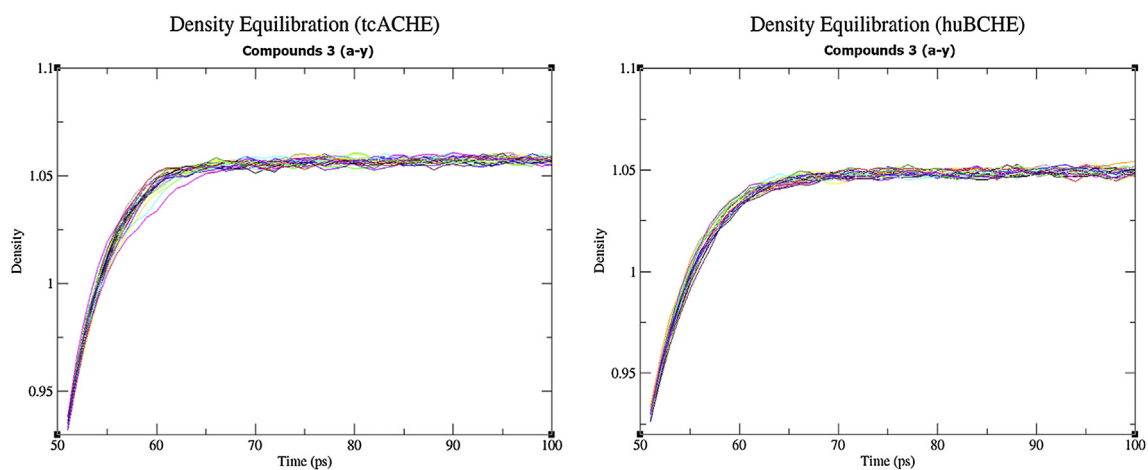


**Fig. 4.** Density plots showing density equilibrations for all individual protein–ligand complexes. Density plots for all compounds during pre-equilibration step for TcAChE complexes (Left). Density plots for all compounds during pre-equilibration step for huBChE complexes (Right).

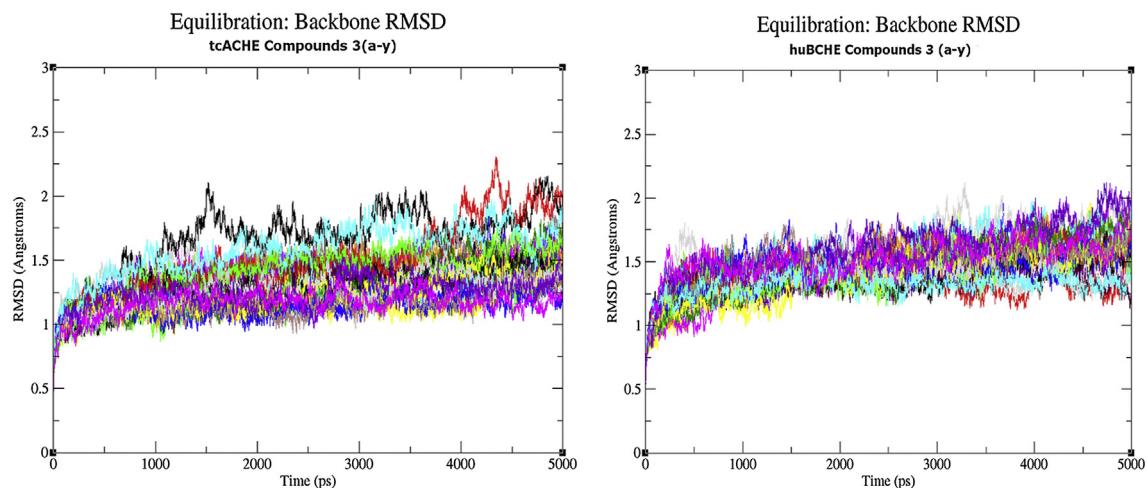


**Fig. 5.** Equilibration plots for all enzyme–ligand complexes of TcAChE and huBChE. RMSD deviations in protein backbone atoms show that the complexes start to equilibrate after 2ns of MD simulation.

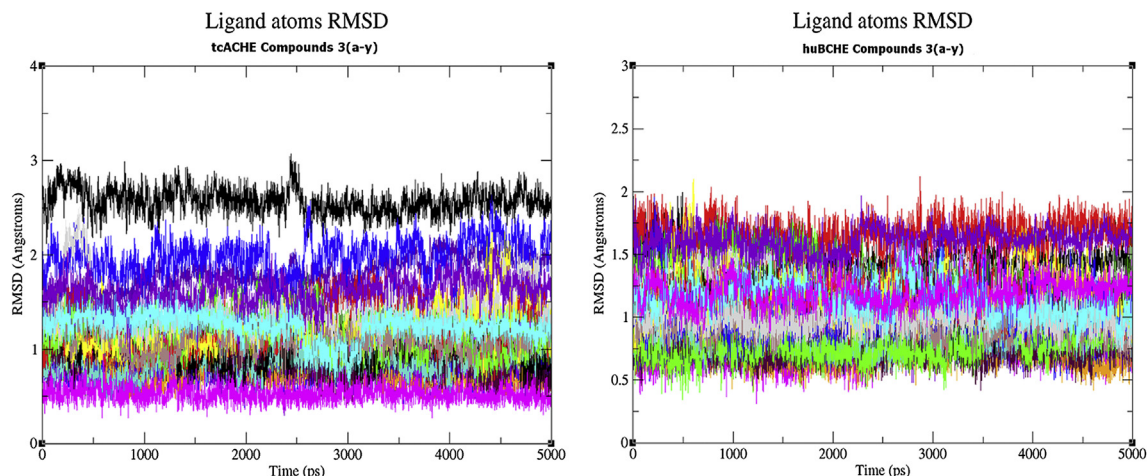


**Fig. 6.** RMSD deviations of ligand atoms during production MD simulation. RMSD plots of ligand atoms during MD simulation of TcAChE complexes (Left). RMSD plots of ligand atoms during MD simulation of huBChE complexes (Right).

### 3. Conclusions

It is evident from the results of cholinesterase assays, cytotoxicity assays and molecular docking studies that some of synthesized cinnamide derivatives are potent inhibitors of cholinesterases as well as effective cytotoxic agents against cancer cell lines (H157). The **3i** demonstrated the best inhibitory potential against EeAChE with the  $IC_{50}$  value of  $0.29 \pm 0.21 \mu\text{M}$  and **3k** showed promising results against hBChE with the  $IC_{50}$  value of  $1.18 \pm 1.31 \mu\text{M}$ . Since phenylcinnamides are reported as effective cytotoxic agents and in the current study we have also showed their anticholinesterase activities therefore the compounds explored in the present

research would help in investigating novel drugs that would act both as anticancer and anticholinesterases inhibitors.

### 4. Experimental

Butyrylcholinesterase (hBChE) (EC 3.1.1.8, from horse serum), *S*-butyrylthiocholine chloride, acetylthiocholine iodide (ATCI), acetylcholinesterase (EeAChE) (EC 3.1.1.7, type VI-S from *electric eel*), 5,5'-dithio-bis(2-nitrobenzoic acid) (DTNB), dimethylsulphoxide (DMSO) and neostigmine methylsulphate, donepezil hydrochloride, chloroform, magnesium sulphate were purchased from Sigma–Aldrich (St. Louis, MO, USA). Tris–HCl,  $\text{MgCl}_2$ ,  $\text{ZnCl}_2$ , RPMI-1640, fetal bovine serum, glutamine, pyruvate, penicillin, streptomycin, and HBSS (Hank's Balanced Salt Solution) were purchased from Sigma–Aldrich, Steinheim, Germany. A lung carcinoma (H157) cell lines were obtained from ATCC (ATCC CRL-5802). Substituted benzaldehydes, malonic acid, pyridine, piperidine, 2,4,6-trichloro-1,3,5 triazine, triethylamine, 3,4,5-trimethoxy aniline and ethyl acetate were purchased from Alfa Aesar (Karlsruhe, Germany).

#### 4.1. General procedure for the synthesis of substituted phenylcinnamide derivatives **3 (a–y)**

Substituted cinnamic acids (**2a–y**) were synthesized by Knoevenagel condensation of corresponding aldehydes (0.01 mol) and monoethyl malonate (0.01 mol) according to literature procedure [30]. A stirred solution of the suitable cinnamic acid (0.01 mol) in acetonitrile was treated with 2,4,6-trichloro-1,3,5-triazine (0.01 mol) and  $\text{Et}_3\text{N}$  (0.02 mol). A slight exotherm ( $1\text{--}2^\circ\text{C}$ ) was observed, and most of the solid was dissolved. The reaction mixture thickened noticeably after 20–40 min. After the mixture was stirred for further 1 h at ambient temperature, the amine reagent (0.02 mol) was added, and a second exotherm of  $2\text{--}4^\circ\text{C}$  was noticed. The reaction mixture was stirred at  $40^\circ\text{C}$  and on completion (TLC examination) was cooled to room temperature and filtered. The solid was washed with a minimal amount of solvent; the filtrates were combined and washed with 1 M sodium hydroxide solution and finally with water. The organic layer was dried over sodium sulphate, and the solvent was removed by vaporation under reduced pressure. The residue was dried under vacuum to yield the amide product and recrystallized from

**Table 3**

Experimental and estimated binding free energy values calculated for all compounds simulated with TcAChE and huBChE enzymes. Experimental free energy values were computed from  $IC_{50}$  values and estimated was calculated by MM/PBSA.

Compound	Experimental $\Delta G$ (kcal/mol)		Estimated $\Delta G$ (kcal/mol) by MM/PBSA	
	TcAChE	huBChE	TcAChE	huBChE
<b>3a</b>	−7.00	−7.30	−16.5532	−16.206
<b>3b</b>	−7.16	−6.08	−9.3075	−15.9281
<b>3c</b>	−6.62	−7.31	−10.9926	−17.1146
<b>3d</b>	−6.61	−6.05	−15.761	−13.2968
<b>3e</b>	−7.05	−6.08	−14.6427	−13.1293
<b>3f</b>	−6.04	−6.06	−9.5405	−14.6314
<b>3g</b>	−6.12	−7.97	−9.2465	−9.1486
<b>3h</b>	−7.82	−6.16	−12.4612	−15.1736
<b>3i</b>	−8.82	−6.07	−22.6499	−19.7891
<b>3j</b>	−5.99	−5.98	−12.8805	−12.0348
<b>3k</b>	−6.03	−8.00	−19.776	−13.7864
<b>3l</b>	−6.61	−6.01	−17.2056	−17.7713
<b>3m</b>	−7.90	−6.22	−12.7105	−9.4361
<b>3n</b>	−5.99	−6.02	−8.8962	−14.5672
<b>3o</b>	−7.41	−6.18	−22.0334	−11.8747
<b>3p</b>	−6.08	−6.20	−15.2873	−13.5464
<b>3q</b>	−6.60	−5.91	−15.1877	−13.5457
<b>3r</b>	−7.03	−7.13	−19.9598	−11.8196
<b>3s</b>	−7.25	−6.91	−16.9283	−11.3597
<b>3t</b>	−5.93	−5.99	−9.624	−13.9076
<b>3u</b>	−6.08	−5.92	−15.8722	−4.8547
<b>3v</b>	−5.99	−6.40	−4.5775	−7.7755
<b>3w</b>	−6.03	−7.94	−17.6119	−13.7757
<b>3x</b>	−7.33	−6.04	−11.2139	−10.0878
<b>3y</b>	−6.98	−6.14	−15.8111	−7.5696

ethanol to afford the products (**3a–y**) in yields mentioned against each.

#### 4.1.1. 3-(3-(Benzyloxy)phenyl)-N-(3,4,5-trimethoxyphenyl)acrylamide (**3a**)

Yield: (75%); R<sub>f</sub>: 0.71 (n-hexane:ethyl acetate, 8:2); m.p. 201 °C; IR: (cm<sup>-1</sup>) 3250–2400 (COOH), 2971(sp<sup>2</sup> CH), 1685 (C=O), 1640 (C=C). <sup>1</sup>H NMR (300 MHz, CDCl<sub>3</sub>): δ 10.5 (s, 1H, NH), 7.40 (m, 5H, Ar–H), 7.16 (dd, 1H, J = 8.1 Hz, 1.2 Hz Ar–H), 6.47 (s, 2H), 6.18 (dd, 1H, J = 8.1 Hz, 1.2 Hz), 7.6 (pseudo triplet, 1H, J = 8.1 Hz), 7.45 (d, 1H, J = 15.6 Hz), 6.30 (d, 1H, J = 15.6 Hz), 5.16 (s, 2H), 4.10 (s, 9H); <sup>13</sup>C NMR (75 MHz, CDCl<sub>3</sub>): δ 165.3, 160.2, 156, 144.9, 137, 136.9, 135.0, 133, 129.36, 128.43, 127.48, 120.8, 116.5, 113.5, 100, 70.8, 60.2. Anal. Calcd for C<sub>25</sub>H<sub>25</sub>NO<sub>5</sub>: C, 71.58; H, 6.01; N, 3.34%; Found: C, 71.54; H, 6.02; N, 3.30%.

#### 4.1.2. 2-Methoxy-4-(3-oxo-3-(3,4,5-trimethoxyphenylamino)prop-1-enyl)phenyl acetate (**3b**)

Yield: (73%); R<sub>f</sub>: 0.66 (n-hexane:ethyl acetate, 8:2); m.p. 215 °C; IR: (cm<sup>-1</sup>) 3270 (NH), (COOH), 3071(sp<sup>2</sup> CH), 1685(C=O), 1470, 1590 (C=C). <sup>1</sup>H NMR (300 MHz, CDCl<sub>3</sub>): δ 10.5 (s, 1H, NH), 7.48 (d, 1H, J = 15.2 Hz), 7.30(s, H, Ar–H), 7.26(d, 1H, J = 8.1 Hz), 7.13(d, 1H, J = 8.1 Hz), 6.47 (s, 2H), 6.40 (d, 1H, J = 15.2 Hz), 4.10 (s, 9H), 3.95 (s, 3H), 2.10 (s, 3H); <sup>13</sup>C NMR (75 MHz, CDCl<sub>3</sub>): δ 165.3, 169.2, 156, 151.9, 144.5, 142.9, 137, 133, 132.0, 129.36, 116.5, 110.9; 100, 60.2, 55.8, 22.5. Anal. Calcd for C<sub>21</sub>H<sub>23</sub>NO<sub>7</sub>: C, 62.84; H, 5.78; N, 3.49%; Found: C, 62.82; H, 5.77; N, 3.51%.

#### 4.1.3. 3-(4-(Acetoxylamino)phenyl)-N-(3,4,5-trimethoxyphenyl)acrylamide (**3c**)

Yield: (78%); R<sub>f</sub>: 0.71 (n-hexane:ethyl acetate, 8:2); m.p. 210 °C; IR: (cm<sup>-1</sup>) 3240 (NH), 3106 (sp<sup>2</sup> CH), 1685 (C=O), 1440, 1633 (C=C). <sup>1</sup>H NMR (300 MHz, CDCl<sub>3</sub>): δ 10.5 (s, 1H, NH), 7.70(d, 2H, J = 8.5 Hz), 7.45 (d, 1H, J = 15.8 Hz), 6.58 (d, 2H, J = 8.5 Hz), 6.47 (s, 2H), 6.40(d, 1H, J = 15.8 Hz) 4.10 (s, 9H), 3.95 (s, 1H, NH), 2.10 (s, 3H), <sup>13</sup>C NMR (75 MHz, CDCl<sub>3</sub>): δ 165.3, 167.2, 156, 150.0, 144.2, 137, 133, 126.5, 120.1, 116.5, 100, 60.2, 26.2. Anal. Calcd for C<sub>20</sub>H<sub>22</sub>N<sub>2</sub>O<sub>6</sub>: C, 62.17; H, 5.74; N, 7.25%; Found: C, 62.14; H, 5.70; N, 7.26%.

#### 4.1.4. 3-(4-(Benzyloxy)-3-methoxyphenyl)-N-(3,4,5-trimethoxyphenyl)acrylamide (**3d**)

Yield:(77%); R<sub>f</sub>: 0.70 (n-hexane:ethyl acetate, 8:2); m.p. 205 °C; IR: (cm<sup>-1</sup>) 3227 (NH), 3020 (sp<sup>2</sup> CH), 1685 (C=O), 1462, 1594 (C=C). <sup>1</sup>H NMR (300 MHz, CDCl<sub>3</sub>): δ 10.5 (s, 1H, NH), 7.45(d, 1H, J = 15.8 Hz), 7.40(m, 5H, Ar–H), 7.25 (s, 1H), 7.20(d, 1H, J = 8.5 Hz), 6.80(d, 1H, J = 8.5 Hz), 6.47 (s, 2H), 6.28(d, 1H, J = 15.8 Hz), 5.16(s, 2H), 4.10 (s, 9H), 4.00 (s, 3H); <sup>13</sup>C NMR (75 MHz, CDCl<sub>3</sub>): δ 165.3, 156, 155.5, 150.2, 144.9, 137, 136.9, 133, 128.5, 127.6, 127.3, 122.5, 116.5, 113.5, 100, 71.8, 60.2, 55.3. Anal. Calcd for C<sub>26</sub>H<sub>27</sub>NO<sub>6</sub>: C, 69.47; H, 6.05; N, 3.12%; Found: C, 69.44; H, 6.02; N, 3.09%.

#### 4.1.5. 3-(3-(Benzyloxy)-4-methoxyphenyl)-N-(3,4,5-trimethoxyphenyl)acrylamide (**3e**)

Yield: (72%); R<sub>f</sub>: 0.45 (n-hexane:ethyl acetate, 8:2); m.p. 208 °C; IR: (cm<sup>-1</sup>) 3233 (NH), 3178 (sp<sup>2</sup> CH), 1685 (C=O), 1462, 1588 (C=C). <sup>1</sup>H NMR (300 MHz, CDCl<sub>3</sub>): δ 10.5 (s, 1H, NH), 7.45(d, 1H, J = 15.8 Hz), 7.40(m, 5H, Ar–H), 7.25 (s, 1H), 7.20(d, 1H, J = 8.5 Hz), 6.80(d, 1H, J = 8.5 Hz), 6.47 (s, 2H), 6.28 (d, 1H, J = 15.8 Hz), 5.16 (s, 2H), 4.10 (s, 9H), 4.01 (s, 3H), <sup>13</sup>C NMR (75 MHz, CDCl<sub>3</sub>): δ 165.3, 156, 155.5, 150.2, 144.9, 137, 136.9, 133, 128.5, 127.6, 127.3, 122.5, 116.5, 113.5, 100, 71.8, 60.2, 55.3. Anal. Calcd for C<sub>26</sub>H<sub>27</sub>NO<sub>6</sub>: C, 69.47; H, 6.05; N, 3.12%; Found: C, 69.44; H, 6.02; N, 3.09%.

#### 4.1.6. 3-(4-(Allyloxy)phenyl)-N-(3,4,5-trimethoxyphenyl)acrylamide (**3f**)

Yield: (71%); R<sub>f</sub>: 0.57 (n-hexane:ethyl acetate, 8:2); m.p. 220 °C; IR: (cm<sup>-1</sup>) 3250 (NH), 3070 (sp<sup>2</sup> CH), 1685 (C=O), 1428, 1608 (C=C). <sup>1</sup>H NMR (300 MHz, CDCl<sub>3</sub>): δ 10.5 (s, 1H, NH), 7.65(d, 2H, J = 7.5 Hz), 7.45 (d, 1H, J = 15.0 Hz), 6.70 (d, 2H, J = 8.1 Hz), 6.47 (s, 2H), 6.30 (d, 1H, J = 15.0 Hz), 6.10(d, 1H, m), 5.40 (dd, 1H, J = 8.1 Hz), 6.40 (d, 1H, J = 5.3 Hz), 4.60 (d, 2H), 4.10 (s, 9H); <sup>13</sup>C NMR (75 MHz, CDCl<sub>3</sub>): δ 165.3, 157.2, 156, 144.2, 137, 133.5, 133, 130.5, 126.5, 120.1, 116.5, 113.2, 100, 70.5, 60.2. Anal. Calcd for C<sub>21</sub>H<sub>23</sub>NO<sub>5</sub>: C, 68.28; H, 6.28; N, 3.79%; Found: C, 68.30; H, 6.25; N, 3.74%.

#### 4.1.7. 3-(3-Oxo-3-(3,4,5-trimethoxyphenylamino)prop-1-enyl)phenyl acetate (**3g**)

Yield: (72%); R<sub>f</sub>: 0.49 (n-hexane:ethyl acetate, 8:2); m.p. 224 °C; IR: (cm<sup>-1</sup>) 3265 (NH), 3171(sp<sup>2</sup> CH), 1685 (C=O), 1420, 1594 (C=C). <sup>1</sup>H NMR (300 MHz, CDCl<sub>3</sub>): δ 10.5 (s, 1H, NH), 7.6 (pseudo triplet, 1H, J = 8.1 Hz), 7.45 (d, 1H, J = 15.0 Hz), 7.38 (dd, 1H, J = 8.1 Hz, 1.2 Hz), 7.28 (s, 1H), 7.18 (dd, 1H, J = 8.1 Hz, 1.2 Hz), 6.47 (s, 2H), 6.30 (d, 1H, J = 15.0 Hz), 4.10 (s, 9H), 2.10 (s, 3H), <sup>13</sup>C NMR (75 MHz, CDCl<sub>3</sub>): δ 165.3, 169.2, 156, 152.3, 144.9, 137, 135.9, 133, 129.2, 128.5, 127.48, 120.8, 116.5, 113.5, 100, 60.2, 20.8. Anal. Calcd for C<sub>20</sub>H<sub>21</sub>NO<sub>6</sub>: C, 64.68; H, 5.70; N, 3.77%; Found: C, 64.63; H, 5.67; N, 3.79%.

#### 4.1.8. 3-(4-(Benzyloxy)-2-hydroxyphenyl)-N-(3,4,5-trimethoxyphenyl)acrylamide (**3h**)

Yield: (74%); R<sub>f</sub>: 0.69 (n-hexane:ethyl acetate, 8: 2), m.p. 2290 °C; IR: (cm<sup>-1</sup>) 3219 (NH), 3080 (sp<sup>2</sup> CH), 1685 (C=O), 1525, 1620 (C=C). <sup>1</sup>H NMR (300 MHz, CDCl<sub>3</sub>): δ 10.5 (s, 1H, NH), 7.60 (d, 1H, J = 15.8 Hz), 7.50 (d, 1H, J = 8.5 Hz), 7.40 (m, 5H, Ar–H), 7.25 (s, 1H), 6.90(d, 1H, J = 8.5 Hz), 6.47 (s, 2H), 6.18 (d, 1H, J = 15.8 Hz), 5.16(s, 2H), 5.0 (s, 1H,OH), 4.10 (s, 9H), 4.00 (s, 3H); <sup>13</sup>C NMR (75 MHz, CDCl<sub>3</sub>): δ 171.5, 162.3, 159.5, 156, 141.9, 137, 136.2, 133, 130.9, 128.5, 127.6, 127.1, 116.5, 113.5, 103.5, 100, 71.8, 60.2. Anal. Calcd for C<sub>25</sub>H<sub>25</sub>NO<sub>6</sub>: C, 68.95; H, 5.79; N, 3.22%; Found: C, 68.91; H, 5.77; N, 3.20%.

#### 4.1.9. 3-(2-(Benzyloxy)phenyl)-N-(3,4,5-trimethoxyphenyl)acrylamide (**3i**)

Yield: (79%); R<sub>f</sub>: 0.63 (n-hexane:ethyl acetate, 8:2); m.p. 233 °C; IR: (cm<sup>-1</sup>) 3258 (NH), 3031 (sp<sup>2</sup> CH), 1685 (C=O), 1474, 1600 (C=C). <sup>1</sup>H NMR (300 MHz, CDCl<sub>3</sub>): δ 10.5 (s, 1H, NH), 7.60 (d, 1H, J = 15.8 Hz), 7.50(m, 4H), 7.40(m, 5H, Ar–H), 6.47 (s, 2H), 6.18 (d, 1H, J = 15.8 Hz), 5.16(s, 2H), 4.10 (s, 9H); <sup>13</sup>C NMR (75 MHz, CDCl<sub>3</sub>): δ 165.3, 155.2, 156, 144.9, 137, 136.9, 135.0, 133, 129.36, 128.43, 127.1, 120.8, 116.5, 113.5, 100, 70.8, 60.2. Anal. Calcd for C<sub>25</sub>H<sub>25</sub>NO<sub>5</sub>: C, 71.58; H, 6.01; N, 3.34%; Found: C, 71.54; H, 6.02; N, 3.30%.

#### 4.1.10. 4-(3-Oxo-3-(3,4,5-trimethoxyphenylamino)prop-1-enyl)phenyl acetate (**3j**)

Yield: (78%); R<sub>f</sub>: 0.66 (n-hexane:ethyl acetate, 8:2); m.p. 205 °C; IR: (cm<sup>-1</sup>) 3297 (NH), 3033 (sp<sup>2</sup> CH), 1685 (C=O), 1500, 1632 (C=C). <sup>1</sup>H NMR (300 MHz, CDCl<sub>3</sub>): δ 10.5 (s, 1H, NH), 7.70 (d, 2H, J = 8.1 Hz), 7.45 (d, 1H, J = 15.0 Hz), 7.30(d, 2H, J = 8.1 Hz), 6.47 (s, 2H), 6.30(d, 1H, J = 15.0 Hz), 4.10 (s, 9H), 2.10 (s, 3H); <sup>13</sup>C NMR (75 MHz, CDCl<sub>3</sub>): δ 169.2, 165.3, 160.3, 156, 144.2, 137, 133.5, 133, 130.5, 126.5, 116.5, 100, 60.2, 20.5. Anal. Calcd for C<sub>20</sub>H<sub>21</sub>NO<sub>6</sub>: C, 64.68; H, 5.70; N, 3.70%; Found: C, 64.72; H, 5.69; N, 3.67%.

#### 4.1.11. 3-(2-Chloro-6-nitrophenyl)-N-(3,4,5-trimethoxyphenyl)acrylamide (**3k**)

Yield: (75%); R<sub>f</sub>: 0.47 (n-hexane:ethyl acetate, 8:2); m.p. 207 °C; IR: (cm<sup>-1</sup>) 3287 (NH), 3089 1(sp<sup>2</sup> CH), 1685 (C=O), 1450, 1595 (C=C). <sup>1</sup>H NMR (300 MHz, CDCl<sub>3</sub>): δ 10.5 (s, 1H, NH), 8.00 (dd, 2H, J = 8.1 Hz, 1.2 Hz), 7.55 (d, 1H, J = 15.0 Hz) 7.45 (pseudo triplet, 1H,

$J = 8.1$  Hz), 7.18 (dd, 1H,  $J = 8.1$  Hz, 1.2 Hz), 6.47 (s, 2H), 6.18 (d, 1H,  $J = 15.0$  Hz), 4.10 (s, 9H);  $^{13}\text{C}$  NMR (75 MHz,  $\text{CDCl}_3$ ):  $\delta$  165.3, 156, 148.2, 145.3, 137, 136.2, 133.5, 133, 130.5, 121.5, 116.5, 100, 60.2. Anal. Calcd for  $\text{C}_{18}\text{H}_{17}\text{ClN}_2\text{O}_6$ : C, 55.04; H, 4.36; N, 7.13%; Found: C, 55.07; H, 4.32; N, 7.14%.

#### 4.1.12. 3-(2-Hydroxy-6-nitrophenyl)-N-(3,4,5-trimethoxyphenyl) acrylamide (**3l**)

Yield: (62%),  $R_f$ : 0.82 (n-hexane:ethyl acetate, 8:2), m.p. 200 °C; IR: ( $\text{cm}^{-1}$ ) 3257 (NH), 3142 ( $\text{sp}^2$  CH), 1685 (C=O), 1473, 1588 (C=C),  $^1\text{H}$  NMR (300 MHz,  $\text{CDCl}_3$ ):  $\delta$  10.5 (s, 1H, NH), 8.00 (dd, 2H,  $J = 8.1$  Hz, 1.2 Hz), 7.55 (d, 1H,  $J = 15.0$  Hz), 7.35 (pseudo triplet, 1H,  $J = 8.1$  Hz), 7.18 (dd, 1H,  $J = 8.1$  Hz, 1.2 Hz), 6.47 (s, 2H), 6.20 (d, 1H,  $J = 15.0$  Hz), 5.0 (s, 1H, OH), 4.10 (s, 9H);  $^{13}\text{C}$  NMR (75 MHz,  $\text{CDCl}_3$ ):  $\delta$  165.3, 159.5, 156, 148.2, 145.3, 137, 136.2, 133, 117.2, 121.5, 116.5, 100, 60.2. Anal. Calcd for  $\text{C}_{25}\text{H}_{25}\text{NO}_5$ : C, 57.75; H, 4.85; N, 7.48%; Found: C, 57.70; H, 4.81; N, 7.46%.

#### 4.1.13. 3-(2-(Allyloxy) phenyl)-N-(3,4,5-trimethoxyphenyl) acrylamide (**3m**)

Yield: (77%),  $R_f$ : 0.44 (n-hexane:ethyl acetate, 8:2), m.p. 210 °C; IR: ( $\text{cm}^{-1}$ ) 3239 (NH), 3074 ( $\text{sp}^2$  CH), 1685 (C=O), 1500, 1609 (C=C).  $^1\text{H}$  NMR (300 MHz,  $\text{CDCl}_3$ ):  $\delta$  10.5 (s, 1H, NH), 7.65 (d, 1H,  $J = 7.5$  Hz), 7.45 (d, 1H,  $J = 15.0$  Hz), 6.90 (2H, m), 6.70 (d, 1H,  $J = 8.1$  Hz), 6.47 (s, 2H), 6.30 (d, 1H,  $J = 15.0$  Hz), 6.10 (d, 1H, m), 5.40 (dd, 1H,  $J = 8.1$  Hz), 6.40 (d, 1H,  $J = 5.3$  Hz), 4.60 (d, 2H), 4.10 (s, 9H);  $^{13}\text{C}$  NMR (75 MHz,  $\text{CDCl}_3$ ):  $\delta$  165.3, 157.2, 156, 147.2, 137, 133.5, 133, 130.5, 125.2, 128.9, 120.1, 117.5, 116.5, 114.2, 100, 70.5, 60.2. Anal. Calcd for  $\text{C}_{21}\text{H}_{23}\text{NO}_5$ : C, 68.28; H, 6.28; N, 3.79%; Found: C, 68.25; H, 6.27; N, 3.77%.

#### 4.1.14. 3-(2,3-Dihydroxyphenyl)-N-(3,4,5-trimethoxyphenyl) acrylamide (**3n**)

Yield: (76%),  $R_f$ : 0.76 (n-hexane:ethyl acetate, 8:2), m.p. 212 °C; IR: ( $\text{cm}^{-1}$ ) 3239 (NH), 3050 ( $\text{sp}^2$  CH), 1685 (C=O), 1467, 1634 (C=C).  $^1\text{H}$  NMR (300 MHz,  $\text{CDCl}_3$ ):  $\delta$  10.5 (s, 1H, NH), 7.45 (d, 1H,  $J = 15.3$  Hz), 7.35 (d, 1H,  $J = 7.5$  Hz), 7.15 (s, 1H), 6.65 (d, 1H,  $J = 7.5$  Hz), 6.47 (s, 2H), 6.30 (d, 1H,  $J = 15.3$  Hz), 5.0 (s, 1H, OH), 4.10 (s, 9H);  $^{13}\text{C}$  NMR (75 MHz,  $\text{CDCl}_3$ ):  $\delta$  165.3, 156, 147.5, 145.2, 144.3, 137, 133, 128.2, 124.3, 117.2, 116.5, 115.5, 100, 60.2. Anal. Calcd for  $\text{C}_{18}\text{H}_{19}\text{NO}_6$ : C, 62.60; H, 5.55; N, 4.06%; Found: C, 62.63; H, 5.52; N, 4.00%.

#### 4.1.15. (3-Nitrophenyl)-N-(3,4,5-trimethoxyphenyl)acrylamide (**3o**)

Yield: (78%),  $R_f$ : 0.26 (n-hexane:ethyl acetate, 8:2); m.p. 232 °C; IR: ( $\text{cm}^{-1}$ ) 3222 (NH), 3065 ( $\text{sp}^2$  CH), 1685 (C=O), 1494, 1598 (C=C).  $^1\text{H}$  NMR (300 MHz, Acetone- $d_6$ ):  $\delta$  10.5 (s, 1H, NH), 8.30 (s, 1H), 8.00 (dd, 1H,  $J = 8.1$  Hz, 1.2 Hz), 7.70 (pseudo triplet, 1H,  $J = 7.55$  (d, 1H,  $J = 15.0$  Hz)), 7.18 (dd, 1H,  $J = 8.1$  Hz, 1.2 Hz), 6.47 (s, 2H), 6.20 (d, 1H,  $J = 15.0$  Hz), 4.10 (s, 9H);  $^{13}\text{C}$  NMR (75 MHz, Acetone- $d_6$ ):  $\delta$  165.3, 156, 147.5, 141.2, 137.2, 137, 134.5, 133, 129.2, 124.3, 123.5, 116.5, 100, 60.2. Anal. Calcd for  $\text{C}_{18}\text{H}_{18}\text{N}_2\text{O}_6$ : C, 60.33; H, 5.06; N, 7.82%; Found: C, 60.30; H, 5.07; N, 7.83%.

#### 4.1.16. 3-(4-Chlorophenyl)-N-(3,4,5-trimethoxyphenyl)acrylamide (**3p**)

Yield: (75%),  $R_f$ : 0.31 (n-hexane:ethyl acetate, 8:2), m.p. 200 °C; IR: ( $\text{cm}^{-1}$ ) 3248 (NH), 3050 ( $\text{sp}^2$  CH), 1685 (C=O), 1453, 1612 (C=C).  $^1\text{H}$  NMR (300 MHz,  $\text{CDCl}_3$ ):  $\delta$  10.5 (s, 1H, NH), 7.60 (d, 2H,  $J = 8.1$  Hz), 7.41 (d, 1H,  $J = 15.0$  Hz), 7.35 (d, 2H,  $J = 8.1$  Hz), 6.47 (s, 2H), 6.30 (d, 1H,  $J = 15.0$  Hz), 4.10 (s, 9H).  $^{13}\text{C}$  NMR (75 MHz,  $\text{CDCl}_3$ ):  $\delta$  165.3, 156, 144.2, 137, 133.5, 133, 132.5, 129.5, 128.5, 116.5, 100, 60.2. Anal. Calcd for  $\text{C}_{18}\text{H}_{18}\text{ClNO}_4$ : C, 62.16; H, 5.22; N, 4.03%; Found: C, 62.18; H, 5.20; N, 4.04%.

#### 4.1.17. 3-(4-Methoxyphenyl)-N-(3,4,5-trimethoxyphenyl) acrylamide (**3q**) [33]

Yield: (72%),  $R_f$ : 0.23 (n-hexane:ethyl acetate, 8:2), m.p. 199 °C; IR: ( $\text{cm}^{-1}$ ) 3282 (NH), 3100 ( $\text{sp}^2$  CH), 1685 (C=O), 1510, 1634 (C=C).  $^1\text{H}$  NMR (300 MHz,  $\text{CDCl}_3$ ):  $\delta$  10.5 (s, 1H, NH), 7.60 (pseudo triplet, 1H,  $J = 8.1$  Hz), 7.55 (d, 1H,  $J = 15.0$  Hz), 7.30 (s, 1H), 7.25 (dd, 1H,  $J = 8.1$  Hz, 1.2 Hz), 6.80 (dd, 1H,  $J = 8.1$  Hz, 1.2 Hz), 6.47 (s, 2H), 6.20 (d, 1H,  $J = 15.0$  Hz), 4.10 (s, 9H), 4.1 (s, 3H);  $^{13}\text{C}$  NMR (75 MHz,  $\text{CDCl}_3$ ):  $\delta$  165.3, 160.5, 156, 141.2, 137.2, 137, 133, 129.2, 120.3, 116.5, 113.5, 112.5, 100, 60.2, 58.9. Anal. Calcd for  $\text{C}_{19}\text{H}_{21}\text{NO}_5$ : C, 66.46; H, 6.16; N, 4.08%; Found: C, 66.43; H, 6.17; N, 4.05%.

#### 4.1.18. 3-(2-Hydroxy-3-methoxyphenyl)-N-(3,4,5-trimethoxyphenyl)acrylamide (**3r**)

Yield: (73%),  $R_f$ : 0.33 (n-hexane:ethyl acetate, 8:2), m.p. 195 °C; IR: ( $\text{cm}^{-1}$ ) 3271 (NH), 3030 ( $\text{sp}^2$  CH), 1685 (C=O), 1447, 1609 (C=C).  $^1\text{H}$  NMR (300 MHz,  $\text{CDCl}_3$ ):  $\delta$  10.5 (s, 1H, NH), 7.55 (d, 1H,  $J = 15.0$  Hz), 7.26 (pseudo triplet, 1H,  $J = 8.1$  Hz), 7.15 (dd, 1H,  $J = 8.1$  Hz, 1.2 Hz), 6.80 (dd, 1H,  $J = 8.1$  Hz, 1.2 Hz), 6.47 (s, 2H), 6.20 (d, 1H,  $J = 15.0$  Hz), 4.10 (s, 9H), 4.1 (s, 3H);  $^{13}\text{C}$  NMR (75 MHz,  $\text{CDCl}_3$ ):  $\delta$  171.5, 156, 137, 133, 150.5, 148.6, 141.2, 122.2, 120.2, 116.5, 113.5, 112.5, 5100, 60.2, 8.9. Anal. Calcd for  $\text{C}_{19}\text{H}_{21}\text{NO}_6$ : C, 63.50; H, 5.89; N, 3.90%; Found: C, 63.48; H, 5.87; N, 3.88%.

#### 4.1.19. 3-(3-Hydroxy-4-methoxyphenyl)-N-(3,4,5-trimethoxyphenyl)acrylamide (**3s**)

Yellow solid (72%),  $R_f$ : 0.37 (n-hexane:ethyl acetate, 8:2), m.p. 222 °C; IR: ( $\text{cm}^{-1}$ ) 3269 (NH), 3120 ( $\text{sp}^2$  CH), 1685 (C=O), 1470, 1630 (C=C).  $^1\text{H}$  NMR (300 MHz, DMSO):  $\delta$  10.5 (s, 1H, NH), 7.45 (d, 1H,  $J = 15.3$  Hz), 7.25 (d, 1H,  $J = 7.5$  Hz), 7.15 (s, 1H), 6.65 (d, 1H,  $J = 7.5$  Hz), 6.47 (s, 2H), 6.30 (d, 1H,  $J = 15.3$  Hz), 5.0 (s, 1H, OH), 4.10 (s, 9H).  $^{13}\text{C}$  NMR (75 MHz, DMSO):  $\delta$  165.3, 156, 148.5, 147.2, 144.3, 1137, 133, 28.2, 124.3, 117.2, 116.5, 115.5, 100, 60.2. Anal. Calcd for  $\text{C}_{19}\text{H}_{21}\text{NO}_6$ : C, 63.50; H, 5.89; N, 3.90%; Found: C, 63.53; H, 5.85; N, 3.91%.

#### 4.1.20. 3-(2,6-Dihydroxyphenyl)-N-(3,4,5-trimethoxyphenyl) acrylamide (**3t**)

Yield: (75%),  $R_f$ : 0.32 (n-hexane:ethyl acetate, 8:2), m.p. 242 °C; IR: ( $\text{cm}^{-1}$ ) 3259 (NH), 3119 ( $\text{sp}^2$  CH), 1685 (C=O), 1470, 1607 (C=C).  $^1\text{H}$  NMR (300 MHz,  $\text{CDCl}_3$ ):  $\delta$  10.5 (s, 1H, NH), 7.55 (d, 1H,  $J = 15.0$  Hz), 7.35 (pseudo triplet, 1H,  $J = 8.1$  Hz), 6.47 (s, 2H), 6.18 (d, 2H,  $J = 8.1$  Hz), 6.20 (d, 1H,  $J = 15.0$  Hz), 3.91 (s, 6H);  $^{13}\text{C}$  NMR (75 MHz,  $\text{CDCl}_3$ ):  $\delta$  165.3, 158.5, 156, 137.2, 137, 133, 129, 116.5, 106.8, 100, 60.2. Anal. Calcd for  $\text{C}_{18}\text{H}_{19}\text{NO}_6$ : C, 62.60; H, 5.55; N, 4.06%; Found: C, 62.62; H, 5.53; N, 4.04%.

#### 4.1.21. 3-(2,3-Dihydroxyphenyl)-N-(3,4,5-trimethoxyphenyl) acrylamide (**3u**)

Yield: (79%),  $R_f$ : 0.30 (n-hexane:ethyl acetate, 8:2), m.p. 234 °C; IR: ( $\text{cm}^{-1}$ ) 3218 (NH), 3075 ( $\text{sp}^2$  CH), 1480, 1610 (C=C);  $^1\text{H}$  NMR (300 MHz,  $\text{CDCl}_3$ ):  $\delta$  10.5 (s, 1H, NH), 7.65 (d, 1H,  $J = 15.0$  Hz), 7.26 (pseudo triplet, 1H,  $J = 8.1$  Hz), 7.15 (dd, 1H,  $J = 8.1$  Hz, 1.2 Hz), 6.80 (dd, 1H,  $J = 8.1$  Hz, 1.2 Hz), 6.47 (s, 2H), 6.20 (d, 1H,  $J = 15.0$  Hz), 4.10 (s, 9H), 3.95 (s, 6H);  $^{13}\text{C}$  NMR (75 MHz,  $\text{CDCl}_3$ ):  $\delta$  165.3, 156, 150.5, 148.6, 145.5, 141.2, 137, 133, 122.2, 120.2, 116.5, 113.5, 61.3, 100, 60.2, 58.9. Anal. Calcd for:  $\text{C}_{18}\text{H}_{19}\text{NO}_6$ : C, 62.60; H, 5.55; N, 4.06%; Found: C, 62.58; H, 5.53; N, 4.05%.

#### 4.1.22. 3-(2,4-Dihydroxyphenyl)-N-(3,4,5-trimethoxyphenyl) acrylamide (**3v**)

Yield: (75%),  $R_f$ : 0.45 (n-hexane:ethyl acetate, 8:2), m.p.: 211 °C; IR: ( $\text{cm}^{-1}$ ) 3254 (NH), 3133 ( $\text{sp}^2$  CH), 1685 (C=O), 1440, 1570 (C=C).  $^1\text{H}$  NMR (300 MHz,  $\text{CDCl}_3$ ):  $\delta$  10.5 (s, 1H, NH), 7.45 (d, 1H,  $J = 15.0$  Hz), 7.15 (d, 1H,  $J = 8.1$  Hz), 6.80 (d, 1H,  $J = 8.1$  Hz), 6.47 (s,

2H), 6.20(d, 1H,  $J = 15.0$  Hz), 6.10 (s, 1H, Ar–H), 5.12 (s, 2H, OH), 4.10 (s, 9H);  $^{13}\text{C}$  NMR (75 MHz,  $\text{CDCl}_3$ ):  $\delta$  165.3, 160.5, 158.6, 156, 145.5, 137, 133, 131.2, 115.2, 116.5, 108.5, 103.5, 100, 60.2. Anal. Calcd for  $\text{C}_{18}\text{H}_{19}\text{NO}_6$ : C, 62.60; H, 5.55; N, 4.06%; Found: C, 62.63; H, 5.52; N, 4.00%.

#### 4.1.23. (E)-3-(2-Chloro-6-fluorophenyl)-N-(3,4,5-trimethoxyphenyl)acrylamide (**3w**)

Yield: (76%);  $R_f$ : 0.62 (n-hexane:ethyl acetate, 8:2), m.p. 231 °C; IR: ( $\text{cm}^{-1}$ ) 3209 (NH), 3090 ( $\text{sp}^2$  CH), 1685 (C=O), 1425, 1525 (C=C).  $^1\text{H}$  NMR (300 MHz,  $\text{CDCl}_3$ ):  $\delta$  10.5 (s, 1H, NH), 7.55(d, 1H,  $J = 15.0$  Hz), 7.15 (m, 3H Ar–H), 6.47 (s, 2H), 6.20(d, 1H,  $J = 15.0$  Hz), 4.10 (s, 9H);  $^{13}\text{C}$  NMR (75 MHz,  $\text{CDCl}_3$ ):  $\delta$  165.3, 158.5, 156, 147.2, 137, 133, 132.8, 130.5, 125.8, 122.6, 116.5, 115.8, 100, 60.2. Anal. Calcd for  $\text{C}_{18}\text{H}_{17}\text{ClFNO}_4$ : C, 59.11; H, 4.68, N, 3.83%; Found: C, 59.13; H, 4.64, N, 3.81%.

#### 4.1.24. 3-(4-(Benzyloxy)-3-methoxyphenyl)-N-(3,4,5-trimethoxyphenyl)acrylamide (**3x**)

Yield: (77%);  $R_f$ : 0.55 (n-hexane:ethyl acetate, 8:2). m.p. 195 °C; IR: ( $\text{cm}^{-1}$ ) 3243 (NH), 3132 ( $\text{sp}^2$  CH), 1685 (C=O), 1495, 1603 (C=C).  $^1\text{H}$  NMR (300 MHz,  $\text{CDCl}_3$ ):  $\delta$  10.5 (s, 1H, NH), 7.60(d, 2H,  $J = 8.5$  Hz), 7.45 (d, 1H,  $J = 15.8$  Hz), 7.40(m, 5H, Ar–H), 6.80 (d, 2H,  $J = 8.5$  Hz), 6.28 (d, 1H,  $J = 15.8$  Hz), 5.16 (s, 2H), 4.10 (s, 9H);  $^{13}\text{C}$  NMR (75 MHz,  $\text{CDCl}_3$ ):  $\delta$  165.3, 160.5, 156, 144.9, 137, 136.9, 133, 130.2, 128.5, 127.6, 127.3, 116.5, 115.5, 100, 70.8, 60.2. Anal. Calcd for  $\text{C}_{25}\text{H}_{25}\text{NO}_5$ : C, 71.58; H, 6.01; N, 3.34%; Found: C, 71.56; H, 6.01; N, 3.33%.

#### 4.1.25. 3-(4-Methoxy-3-nitrophenyl)-N-(3,4,5-trimethoxyphenyl)acrylamide (**3y**)

Yield: (76%);  $R_f$ : 0.56 (n-hexane:ethyl acetate, 8:2), m.p. 202 °C; IR: ( $\text{cm}^{-1}$ ) 3278 (NH), 3121 ( $\text{sp}^2$  CH), 1421, 1610 (C=C).  $^1\text{H}$  NMR (300 MHz,  $\text{CDCl}_3$ ):  $\delta$  10.5 (s, 1H, NH), 8.15(s, 1H), 8.10(d, 1H,  $J = 7.5$  Hz), 7.45 (d, 1H,  $J = 15.3$  Hz), 7.30 (d, 1H,  $J = 7.5$  Hz), 6.47 (s, 2H), 6.30 (d, 1H,  $J = 15.3$  Hz), 4.10 (s, 9H), 4.0 (s, 1H,  $\text{CH}_3$ );  $^{13}\text{C}$  NMR (75 MHz,  $\text{CDCl}_3$ ):  $\delta$  165.3, 156, 155.3, 149.5, 144.3, 137, 136.2, 133, 130.3, 121.2, 117.2, 116.5, 100, 60.3, 60.2. Anal. Calcd for  $\text{C}_{19}\text{H}_{20}\text{N}_2\text{O}_7$ : C, 58.76; H, 5.19; N, 7.21%; Found: C, 58.74; H, 5.16; N, 7.22%.

### 4.2. In vitro inhibitory studies on EeAChE and hBChE

Ellman's method was used to evaluate the inhibitory activities of phenylcinnamide derivatives against EeAChE and hBChE [34]. The compounds studied were first dissolved in DMSO (end concentration of DMSO was 1% in the assay) and studied at a 0.5 mM final concentration for initial screening. The compounds exhibiting more than 50% inhibition were further tested by making eight to ten serial dilutions in assay buffer (50 mM Tris–HCl, 0.1 M NaCl and 0.02 M  $\text{MgCl}_2$ , pH 8.0). Composition of the reaction mixture was: 20  $\mu\text{L}$  assay buffer, 10  $\mu\text{L}$  of test compound and 10  $\mu\text{L}$  of enzymes (0.5 and 3.4 U/mg of EeAChE or hBChE, respectively). A 10 min pre-incubation of the reaction mixture at 25 °C was carried out. At the end of the pre-incubation period, 10  $\mu\text{L}$  of 1 mM acetylthiocholine iodide or butyrylthiocholine chloride were added to the respective EeAChE or hBChE enzyme solution to start the enzymatic reactions. The mixtures were incubated for 15 min at 25 °C. The change in the absorbance was measured at 405 nm to determine the amount of the product using a microplate reader (Bio-Tek ELx800™). Neostigmine and donepezil were used as standard inhibitors. Assays were performed with a blank containing all of the components except enzyme or substrate in order to account for a non-enzymatic reaction. Each concentration was analyzed in triplicate. Enzyme dilution buffer consisted of 50 mM Tris–HCl buffer containing 0.1% (w/v) bovine serum albumin (BSA) and pH 8.0. The linear

regression parameters were determined for each curve and the  $\text{IC}_{50}$  values were measured. The computer program GraphPad Prism 5.0 (San Diego, CA, USA) was used to analyze the data.

### 4.3. Cell lines and cultures

Lung carcinoma (H157) cell lines (ATCC CRL-5802) were kept in RPMI-1640 [having heat-inactivated fetal bovine serum (10%) glutamine (2 mM), Pyruvate (1 mM), 100 U/mL penicillin and 100  $\mu\text{g}/\text{mL}$  streptomycin] in T-75  $\text{cm}^2$  sterile tissue culture flasks in a 5%  $\text{CO}_2$  incubator at 37 °C [35]. 6-well plates were used for growing H157 cells by inoculating  $10^4$  cells per 100  $\mu\text{L}$  per well. For experiments, H157 were grown in 96-well plates by inoculating  $10^4$  cells/100  $\mu\text{L}$ /well, and plates were incubated at 37 °C in a 5%  $\text{CO}_2$  incubator. Within 24 h, a uniform monolayer was formed which was used for experiments.

#### 4.3.1. Cytotoxicity analysis by sulforhodamine B (SRB) assays

To perform cytotoxicity assay with H157 cells, a previously described method by Skehan et al. [36] was adopted with some modifications. Briefly, H157 cells were cultured in different 96 well plates for 24 h. The compounds in different concentrations (100, 50, 25 and 1  $\mu\text{M}$ ) were inoculated in test wells while control and blank wells were also prepared containing standard drug (VCN) and culture media with cells respectively. The plates were then incubated for 48 h. After that cells were fixed with 50  $\mu\text{L}$  of 50% ice cold TCA solution at 4 °C for 1 h. The plates were washed 5 times with PBS and air dried. Fixed cells were further treated with 0.4% w/v sulforhodamine B dye prepared in 1% acetic acid solution and left at room temperature for 30 min. After that the plates were rinsed with 1% acetic acid solution and allowed to dry. In order to solubilize the dye, the dried plates were treated with 10 mM Tris base solution for 10 min at room temperature. Absorbance was measured at 490 nm subtracting the background measurement at 630 nm [37].

### 4.4. Molecular modelling studies of cholinesterases

#### 4.4.1. Structure selection and preparation

Molecular modelling studies were conducted to observe the interactions and selectivity of the compounds against both AChE and BChE enzymes. In order to perform efficient modelling studies, high-resolution structures of both enzymes were selected from the Protein DataBank [38] and prepared for the modelling. A high-resolution crystal structure of 2.19 Å from *T. californica* (PDB Code: 3I6Z) was selected for acetylcholinesterase (TcAChE) and a high-resolution crystal structure of 2.00 Å from human (PDB Code: 1P0I) was selected for human butyrylcholinesterase (huBChE). Both structures have well defined binding sites, as the X-Ray structures for both enzymes are co-crystallized with bound inhibitors. The TcAChE was co-crystallized with Galantamine (PDB ID: G6X) and huBChE was co-crystallized with bound ligands Butanoic acid (PDB ID: BUA) and Glycerol (PDB ID: GOL) that occupy the binding site of the enzyme.

Before studying the proteins in molecular modelling experiments, the structures of enzymes and compounds were prepared. The enzyme structures were protonated with Protonate3D [39] algorithm implemented in the molecular modelling tool MOE [40]. Missing atoms of some residues were completed with utility programs built-in in AmberTools-1.5 [41] package. The structures were energy minimized using Amber99 force field with all the heteroatoms and solvent molecules present in the protein. The backbone atoms were restrained with a small force in order to avoid collapse of the binding pockets during energy minimization

calculations. After minimization, the co-crystallized ligands and solvent molecules were removed.

#### 4.4.2. Compounds preparation

The 3D structural coordinates of the compounds were generated for all the compounds using MOE followed by assignment of protonation and ionization states in physiological pH range by using the “wash” module. Afterwards, the compounds' structures were energy minimized with the MMFF94x force field for the docking studies. For molecular dynamics simulations, the compound structures were prepared by using antechamber program present in AmberTools, to derive AM1-BCC charges and force field parameters for the individual compounds.

#### 4.4.3. Docking studies

For the docking studies, the binding sites of both enzymes were defined by including residues surrounding the co-crystallized ligand in 7.5 Å radius. The default docking and scoring parameters were chosen for the docking calculations and the top 10 docked conformations based on docking scores were retained for analyzing the interactions and binding modes. In order to make sure that the protein structure is prepared well for docking, the co-crystallized bound ligands were re-docked and the same binding modes were reproduced with an RMSD less than 1.8 Å for the 7th ranking conformation for galantamine re-docked to TcAChE. A re-docking experiment was also performed with huBChE by first aligning its X-ray structure to that of TcAChE and then using galantamine as a reference ligand in huBChE.

#### 4.4.4. Pose ranking

The docked poses of each compound were evaluated for favourable interactions with the enzymes and pose ranking and selection for each docked conformation of the compound was performed by using an external scoring function, NNScore that evaluates and predicts the most favourable conformation (pose) among a set of different poses of the same ligand.

#### 4.4.5. Molecular dynamics simulations

Molecular dynamics (MD) simulations were performed on the ligand-docked structures of TcAChE and huBChE inhibitor complexes. The aim of MD studies was to evaluate the stability of the docked binding modes as well as to determine the free energies of binding for the docked conformations of the compounds. The protonated enzyme structures were subsequently parameterized for MD simulations. The force field charges for the protein structures were derived by using Amber [41] force field ff99SB. The force field charges and parameters for the compounds were derived using Antechamber module of Amber. AM1-BCC charges were used for the ligands calculated by the Antechamber and the parameters for the ligands were adapted from the general amber force field (GAFF) library. The docked enzyme–ligand complexes were solvated using the Leap module of Amber by using an octahedron box of the TIP3P water model with a distance of 8 Å between the edge of the box and the protein. The solvated complexes were neutralized by using counter chloride or sodium ions to neutralize the negatively charged protein–ligand complexes. Each individual enzyme–ligand solvated complex system was minimized with 2500 steps of conjugate gradient minimization followed by 2500 steps of steepest decent minimization.

After minimization, the protein–ligand complex systems were equilibrated before running the MD simulations to avoid any instability during the production MD runs. The equilibration steps included 50ps of gradual heating (from 0 to 300 K temperature) with NMR option, 50ps of density equilibration with weak restraints on the complex atoms followed by 5ns of constant pressure

equilibration at 300 K. The equilibration process was carried out using Sander program of Amber12 package. Molecular dynamics simulations were performed by using Particle Mesh Ewald (PME) MD program of Amber12 package on the equilibrated complexes. With a step size of 2fs, the production MD simulations were performed for 5ns time scale and atomic coordinates after each 500 step were recorded. The SHAKE algorithm was applied to constrain bonds involving hydrogen atoms with 8 Å van der Waals cut off using the PME method.

#### 4.4.6. Calculation of binding free energy

The binding free energies were estimated by using Mechanics/Poisson–Boltzmann Surface Area (MM/PBSA) and Molecular Mechanics/Generalized Born Surface Area (MM/GBSA) calculations. MM/PBSA and MM/GBSA based energies were calculated for the snapshots extracted from the 5ns MD trajectories that included 5000 snapshots recorded at 1ps time interval. The interaction energies and salvation free energies were computed for the complex, receptor and ligand at each 5th snapshot in the trajectory to obtain statistically significant results. In order to correlate the estimated binding energy values, the experimental IC<sub>50</sub> values were first transformed to ΔG by the following formula:

$$\Delta G = -RT \ln K_i$$

where R is gas constant, T is temperature in Kelvin (295 K) and K<sub>i</sub> (in nM) is the experimental affinity value. A comparison of estimated binding energy values calculated by both MM/PBSA and MM/GBSA methods with that of experimental ΔG values for the compounds was carried out to observe correlation between the predicted and experimentally determined values.

#### Acknowledgement

This work was financially supported by COMSTECH–TWAS and German–Pakistani Research Collaboration Programme.

#### Appendix A. Supplementary data

Supplementary data related to this article can be found at <http://dx.doi.org/10.1016/j.ejmech.2014.03.015>.

#### References

- [1] Y. Shen, J. Zhang, R. Sheng, X. Dong, Q. He, B. Yang, Y. Hu, Synthesis and biological evaluation of novel flavonoid derivatives as dual binding acetylcholinesterase inhibitors, *Journal of Enzyme Inhibition and Medicinal Chemistry* 24 (2009) 372–380.
- [2] P. Zelík, A. Lukešová, L.N. Voloshko, D. Štys, J. Kopecký, Screening for acetylcholinesterase inhibitory activity in cyanobacteria of the genus *Nostoc*, *Journal of Enzyme Inhibition and Medicinal Chemistry* 24 (2009) 531–536.
- [3] D.H. Small, S. Mok, J.C. Bornstein, Alzheimer's disease and Abeta toxicity: from top to bottom, *Nature Reviews Neuroscience* 2 (2001) 595–598.
- [4] G. Waldemar, B. Dubois, M. Emre, J. Georges, I.G. McKeith, M. Rossor, P. Scheltens, P. Tariska, B. Winblad, Recommendations for the diagnosis and management of Alzheimer's disease and other disorders associated with dementia: EFNS guideline, *European Journal of Neurology* 14 (2007) e1–26.
- [5] M.H. Tabert, X. Liu, R.L. Doty, M. Serby, D. Zamora, G.H. Pelton, K. Marder, M.W. Albers, Y. Stern, D.P. Devanand, A 10-item smell identification scale related to risk for Alzheimer's disease, *Annals of Neurology* 58 (2005) 155–160.
- [6] A.V. Terry, J.J. Buccafusco, The cholinergic hypothesis of age and Alzheimer's disease-related cognitive deficits: recent challenges and their implications for novel drug development, *Journal of Pharmacology and Experimental Therapeutics* 306 (2003) 821–827.
- [7] C.P. Ferri, M. Prince, C. Brayne, H. Brodaty, L. Fratiglioni, M. Ganguli, K. Hall, K. Hasegawa, H. Hendrie, Y. Huang, A. Jorm, C. Mathers, P.R. Menezes, E. Rimmer, M. Sczufca, Global prevalence of dementia: a Delphi consensus study, *Lancet* 366 (2005) 2112–2117.
- [8] A.V. Maltsev, S. Bystryak, O.V. Galzitskaya, The role of beta-amyloid peptide in neurodegenerative diseases, *Ageing Research Reviews* 10 (2011) 440–452.

- [9] M. Pohanka, Cholinesterases, a target of pharmacology and toxicology, *Biomedical Papers* 155 (2011) 219–229.
- [10] G. Gibney, S. Camp, M. Dionne, K. MacPhee-Quigley, P. Taylor, Mutagenesis of essential functional residues in acetylcholinesterase, *Proceedings of the National Academy of Sciences of the United States of America* 87 (1990) 7546–7550.
- [11] M. Ekholm, H. Kanschijn, Comparative model building of human butyrylcholinesterase, *Journal of Molecular Structure: THEOCHEM* 467 (1999) 161–172.
- [12] A. Ordentlich, D. Barak, C. Kronman, N. Ariel, Y. Segall, B. Velan, A. Shafferman, Functional characteristics of the oxyanion hole in human acetylcholinesterase, *Journal of Biological Chemistry* 273 (1998) 19509–19517.
- [13] D.C. Vellom, Z. Radic, Y. Li, N.A. Pickering, S. Camp, P. Taylor, Amino acid residues controlling acetylcholinesterase and butyrylcholinesterase specificity, *Biochemistry* 32 (1993) 12–17.
- [14] P. Taylor, S. Lappi, Interaction of fluorescence probes with acetylcholinesterase. Site and specificity of propidium binding, *Biochemistry* 14 (1975) 1989–1997.
- [15] D. Barak, C. Kronman, A. Ordentlich, N. Ariel, A. Bromberg, D. Marcus, A. Lazar, B. Velan, A. Shafferman, Acetylcholinesterase peripheral anionic site degeneracy conferred by amino acid arrays sharing a common core, *Journal of Biological Chemistry* 269 (1994) 6296–6305.
- [16] M. Bartolini, C. Bertucci, V. Cavrini, V. Andrisano,  $\beta$ -Amyloid aggregation induced by human acetylcholinesterase: inhibition studies, *Biochemical Pharmacology* 65 (2003) 407–416.
- [17] N.C. Inestrosa, A. Alvarez, C.A. Perez, R.D. Moreno, M. Vicente, C. Linker, O.I. Casanueva, C. Soto, J. Garrido, Acetylcholinesterase accelerates assembly of amyloid- $\beta$ -peptides into Alzheimer's fibrils: possible role of the peripheral site of the enzyme, *Neuron* 16 (1996) 881–891.
- [18] R. Raza, A. Saeed, M. Arif, S. Mahmood, M. Muddassar, A. Raza, J. Iqbal, Synthesis and biological evaluation of 3-thiazolocoumarinyl Schiff-base derivatives as cholinesterase inhibitors, *Chemical Biology & Drug Design* 80 (2012) 605–615.
- [19] E. Giacobini, Cholinesterase inhibitors: new roles and therapeutic alternatives, *Pharmacological Research* 50 (2004) 433–440.
- [20] M. Weinstock, Selectivity of cholinesterase inhibition: clinical implications for the treatment of Alzheimer's disease, *CNS drugs* 12 (1999) 307–323.
- [21] P. Taylor, Cholinergic Agonists, Goodman and Gilman's the Pharmacological Basis of Therapeutics, sixth ed., Macmillan, New York, 1980, pp. 91–99.
- [22] X. Zhou, X.-B. Wang, T. Wang, L.-Y. Kong, Design, synthesis, and acetylcholinesterase inhibitory activity of novel coumarin analogues, *Bioorganic & Medicinal Chemistry* 16 (2008) 8011–8021.
- [23] P.D. Greenspan, A.J. Main, S.S. Bhagwat, L.I. Barsky, R.A. Doti, A.R. Engle, L.M. Frey, H. Zhou, K.E. Lipson, M.H. Chin, N-aryl cinnamides: a novel class of rigid and highly potent leukotriene B<sub>4</sub> receptor antagonists, *Bioorganic & Medicinal Chemistry Letters* 7 (1997) 949–954.
- [24] A. Ford-Hutchinson, Leukotriene B<sub>4</sub> in inflammation, *Critical Reviews in Immunology* 10 (1990) 1.
- [25] J. Grabbe, B.M. Czarnetzki, T. Rosenbach, M. Mardin, Identification of chemotactic lipoxigenase products of arachidonate metabolism in psoriatic skin, *Journal of Investigative Dermatology* 82 (1984) 477–479.
- [26] K. Yoshimura, S. Nakagawa, S. Koyama, T. Kobayashi, T. Homma, Leukotriene B<sub>4</sub> induces lung injury in the rabbit: role of neutrophils and effect of indomethacin, *Journal of Applied Physiology* 74 (1993) 2174–2179.
- [27] N. Clapp, M. Henke, R. Hansard, R. Carson, D. Widomski, C. Anglin, R. Walsh, S. Djuric, D. Fretland, Anti-inflammatory activity of the leukotriene B<sub>4</sub> receptor antagonist, SC-41930, in colitic cotton-top tamarins, *Agents and Actions* 41 (1994) C254–C255.
- [28] N. Ahmadzadeh, M. Shingu, M. Nobunaga, T. Tawara, Relationship between leukotriene B<sub>4</sub> and immunological parameters in rheumatoid synovial fluids, *Inflammation* 15 (1991) 497–503.
- [29] A. Cavalli, M.L. Bolognesi, A. Minarini, M. Rosini, V. Tumiatti, M. Recanatini, C. Melchiorre, Multi-target-directed ligands to combat neurodegenerative diseases, *Journal of Medicinal Chemistry* 51 (2008) 347–372.
- [30] J. Lu, P.H. Toy, Organocatalytic decarboxylative Doebner-Knoevenagel reactions between arylaldehydes and monoethyl malonate mediated by a bifunctional polymeric catalyst, *Synlett* (2011) 1723–1726.
- [31] K. Tanaka, K. Matsuo, A. Nakanishi, T. Hatano, H. Izeki, Y. Ishida, W. Mori, Syntheses and anti-inflammatory and analgesic activities of hydroxamic acids and acid hydrazides, *Chemical & Pharmaceutical Bulletin (Tokyo)* 31 (1983) 2810–2819.
- [32] H.L. Rayle, L. Fellmeth, Development of a process for triazine-promoted amidation of carboxylic acids, *Organic Process Research & Development* 3 (1999) 172–176.
- [33] R.S. Dohager, K.S. Putt, B.J. Allen, B.J. Leslie, V. Nesterenko, P.J. Hergenrother, Synthesis and identification of small molecules that potentially induce apoptosis in melanoma cells through G1 cell cycle arrest, *Journal of the American Chemical Society* 127 (2005) 8686–8696.
- [34] G.L. Ellman, K.D. Courtney, V. Andres Jr., R.M. Feather-Stone, A new and rapid colorimetric determination of acetylcholinesterase activity, *Biochemical Pharmacology* 7 (1961) 88–95.
- [35] K. Araki-Sasaki, S. Aizawa, M. Hiramoto, M. Nakamura, O. Iwase, K. Nakata, Y. Sasaki, T. Mano, H. Handa, Y. Tano, Substance P-induced cadherin expression and its signal transduction in a cloned human corneal epithelial cell line, *Journal of Cellular Physiology* 182 (2000) 189–195.
- [36] P. Skehan, R. Storeng, D. Scudiero, A. Monks, J. McMahon, D. Vistica, J.T. Warren, H. Bokesch, S. Kenney, M.R. Boyd, New colorimetric cytotoxicity assay for anticancer-drug screening, *Journal of the National Cancer Institute* 82 (1990) 1107–1112.
- [37] G.S. Longo-Sorbello, G. m Say, D. Banerjee, J.R. Bertino, Cytotoxicity and Cell Growth Assays, in: *Cell Biology, Four-volume Set: a Laboratory Handbook*, vol. 1, 2005, p. 315.
- [38] D.S. Goodsell, Computational docking of biomolecular complexes with Auto-Dock, *Cold Spring Harbor Protocols* 2009 (2009) pdb prot5200.
- [39] P. Labute, Protonate 3D, 2007. <http://www.chemcomp.com/journal/proton.htm>.
- [40] MOE (The Molecular Operating Environment) Version 2010.10, Chemical Computing Group Inc. <http://www.chemcomp.com>.
- [41] D.A. Case, T. Darden, T.E. Cheatham III, C.L. Simmerling, J. Wang, R.E. Duke, R. Luo, M. Crowley, R.C. Walker, W. Zhang, K.M. Merz, B. Wang, S. Hayik, A. Roitberg, G. Seabra, I. Kolossvary, K.F. Wong, F. Paesani, J. Vanicek, X. Wu, S.R. Brozell, T. Steinbrecher, H. Gohlke, L. Yang, C. Tan, J. Mongan, V. Hornak, G. Cui, D.H. Mathews, M.G. Seetin, C. Sagui, V. Babin, P.A. Kolman, AMBER11, University of California, San Francisco, 2010.